

## Deep Etching of Silicon Based on Metal-Assisted Chemical Etching

Anafi Nur'aini and Ilwhan Oh\*

Cite This: *ACS Omega* 2022, 7, 16665–16669

Read Online

ACCESS |



Metrics &amp; More

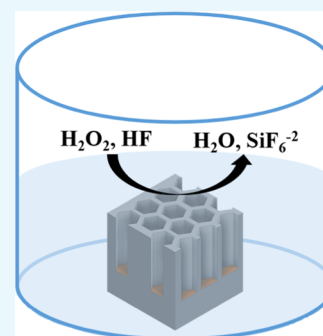


Article Recommendations



Supporting Information

**ABSTRACT:** A deep etching method for silicon “micro”structures was successfully developed. This wet etching process is based on metal-assisted chemical etching (MACE), which was previously mainly utilized to etch the features that have lateral dimensions of “nanometers.” In this novel MACE, the critical improvement was to promote the “out-of-plane” mass transfer at the metal/Si interface with an ultrathin metal film. This enabled us to etch micrometer-wide holes, which was previously challenging due to the mass transport limitation. In addition, it was found that when ethanol was used as a solvent instead of water, the formation of porous defects was suppressed. Under the optimized etch conditions, deep (>200 μm) and vertical (>88°) holes could be carved out at a fast etch rate (>0.4 μm/min). This novel deep MACE will find utility in applications such as microelectromechanical systems (MEMS) devices or biosensors.



## 1. INTRODUCTION

Silicon micromachining is a technology to fabricate various micro- or nanostructures on a silicon substrate through deep etching.<sup>1</sup> Silicon micromachining is used in various applications such as vertical flash memory, microelectromechanical systems (MEMS) devices, and biosensors. In general, silicon micromachining can be classified into two categories. The first category is dry etching. In most practices, deep reactive ion etch (DRIE) is used to fabricate high aspect ratio structures on silicon substrates. This method has advantages in that the etching rate is fast and the etch profile is clean. However, disadvantages are the high cost of the DRIE equipment and the formation of a residual film after the process. The second category is wet etching in a liquid etchant. Compared to dry etching, the process cost of wet etching is low, but the etching rate is relatively slow, and limitations exist in the etch profile that can be produced by a specific wet etch recipe. For example, alkaline etching of Si at an elevated temperature produces an anisotropic profile with the Si(111) surface.<sup>2</sup> However, recent advances in Si wet etching have led to improved performances. For example, Cozzi et al. reported silicon electrochemical etching (ECE), which shows an etching rate faster than the dry etch process.<sup>3</sup>

The most recently developed Si wet etching method is metal-assisted chemical etch (MACE).<sup>4–6</sup> In traditional etching, the substrate area where the pattern (that is, the etch mask) is present is protected from etching, and the area that is exposed to the etchant is etched. In contrast, MACE exhibits a peculiar phenomenon in which the area covered by the metal pattern is etched. This is because the metal layer functions as a catalyst to reduce oxidation and supplies holes to the underlying Si substrate.<sup>7</sup>

The principle of metal-assisted chemical etching is shown in Figure 1. A thin metal layer is deposited on the Si substrate and

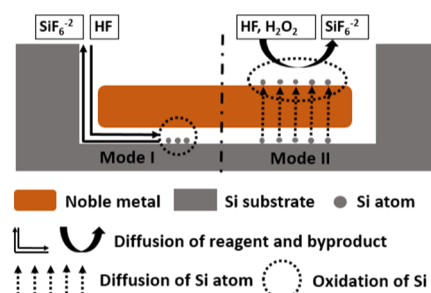
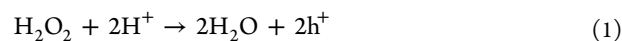


**Figure 1.** Schematic diagram of metal-assisted chemical etching (MACE).  $\text{H}_2\text{O}_2$  and HF as reactants and the metal layer as a catalyst. The reduction of  $\text{H}_2\text{O}_2$  produces holes, which then oxidize the Si layer.

patterned by photolithography. Typically, noble metals such as Ag,<sup>7,8</sup> Au,<sup>9</sup> Pd,<sup>10,11</sup> and Pt<sup>11</sup> are utilized as a catalyst. Then, the patterned substrate is immersed in a mixture of an oxidizing agent (hydrogen peroxide) and an etchant (hydrofluoric acid).

The metal layer on the silicon substrate functions as a catalyst and cathode at the same time. On the metal catalyst, hydrogen peroxide ( $\text{H}_2\text{O}_2$ ) is reduced to generate holes.



These holes are diffused through the metal layer and injected into the silicon substrate, which acts as an anode. Si is

**Received:** February 24, 2022

**Accepted:** April 5, 2022

**Published:** May 2, 2022



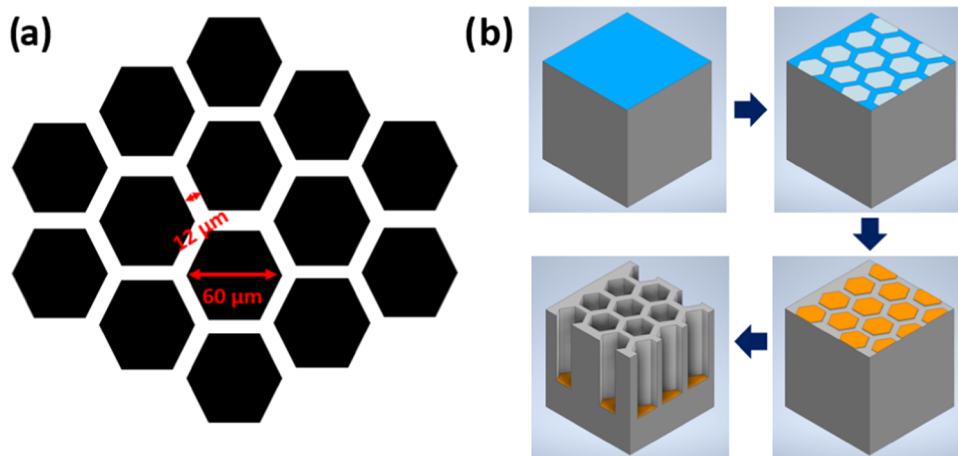
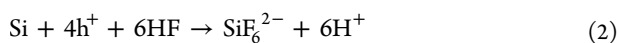


**Figure 2.** (a) Mask design for the metal pattern. The white part is lifted, leaving a honeycomb pattern on the metal layer. The diameter of each hexagon is  $60\ \mu\text{m}$ , and the space is  $12\ \mu\text{m}$ . (b) Schematic of macropore fabrication, including wafer cleaning, lithography, metal deposition, and lift-off, followed by wet metal-assisted chemical etching (MACE).

oxidized by the injected holes and dissolved at the Si/metal interface by hydrofluoric acid (HF) in the following reaction



Note that **reaction 2** occurs at the interface between the Si substrate and the overlying metal layer, which means that the overlying metal film will hinder the mass transfer of reactants and products. For a relatively thick metal layer ( $>50\ \text{nm}$ ), the maximum mass transfer occurs in the in-plane mode. That is, the reaction products should diffuse along with the extremely thin space between the metal and the substrate before escaping through the edge of the metal layer (Mode I in **Figure 1**). This is the reason why the MACE process has been adopted mostly to fabricate nanostructures, where the in-plane mass transfer is much easier. However, for the “micro”structures, the in-plane mass transfer takes so long that nonuniform etching occurs along the metal layer.<sup>7</sup>

As the “in-plane” mass transfer is too slow to etch the metal films with a micrometer dimension, it is devised that enhancing the “out-of-plane” mass transfer (Mode II in **Figure 1**) can be a solution. When the metal layer becomes extremely thin ( $<10\ \text{nm}$ ), numerous pinholes in the ultrathin metal layer should promote the out-of-plane mass transfer of reactants and products across the metal-covered substrate. In fact, our previous report showed that the etch rate in MACE was significantly enhanced for ultrathin metal layers ( $3\text{--}10\ \text{nm}$ ).<sup>9</sup> More recently, Kim et al. showed that the MACE of Si microstructures having lateral dimensions from  $5\ \mu\text{m}$  up to millimeters is possible with an ultrathin metal layer ( $5\text{--}10\ \text{nm}$ ).<sup>12</sup> They found that the Au/Ag bilayer configuration leads to a quite stable etch reaction upon a prolonged etch duration of up to  $>5\ \text{h}$ . In another report involving deep etching of  $50\ \mu\text{m}$ -width features, Miao et al. found that the silicon substrate can be etched with smooth sidewalls with an etchant solution containing ethanol, instead of the conventional aqueous-based solution.<sup>13</sup>

In this work, we customized and optimized the conventional MACE process, with which the etching of features having lateral dimensions exceeding micrometers was not feasible due to the mass transfer limitations. We showed that by enhancing the out-of-plane mass transfer with an ultrathin permeable metal film, the features with lateral dimensions exceeding tens

of micrometers can be fabricated by the customized MACE. Furthermore, to minimize the formation of a porous layer and maximize the etching rate, the etching solution composition was optimized with respect to the nature of the metal layer and the solvent. The customized MACE process, which can fabricate a high aspect ratio Si structure with lateral dimensions exceeding tens of micrometers up to millimeters, will find its utility in microelectromechanical systems (MEMSs) and micro total analysis system ( $\mu\text{TAS}$ ) applications.

## 2. EXPERIMENTAL SECTION

In this work, we have carried out a MACE process on a silicon wafer (p-type;  $10\ \Omega\cdot\text{cm}$ ) patterned by photolithography. The mask design for a mesh pattern is shown in **Figure 2**. This mask was used to create a metal pattern on the silicon wafer through the lift-off process. The design looks like a honeycomb with a hexagonal diameter of  $60\ \mu\text{m}$ , and the space between each hexagon is  $12\ \mu\text{m}$ .

For the lift-off process, a photoresist was spin-coated on the Si wafer and patterned using the mask, as shown in **Figure 2b**. After UV exposure and development, the patterned Si was cleaned by dipping in a buffered oxide etchant (BOE). A single or double metal layer was deposited using an e-beam evaporator. Subsequently, the photoresist was lifted off, leaving the desired metal patterns.

The MACE process began briefly by dipping the sample in 50% HF for 20 s to remove the native oxide in the Si surface. After rinsing with distilled water and drying with  $\text{N}_2$  gas, the Si was immersed in the etching solution, which contained 5–8 M HF and 0.2–0.8 M  $\text{H}_2\text{O}_2$ . The solvent for the etching solution was distilled water, ethanol, or water/ethanol mixed solution (60–80% (v/v) ethanol). A medium-sized ( $\sim 2\ \text{L}$ ) etching bath was utilized so that even after extended etching the consumption of reagents was minimal ( $<2\%$ ). After immersing for varied hours, the sample was sonicated in distilled water for 10 min. All etching processes were conducted at room temperature with no stirring. For characterization of the etch results, scanning electron microscopes (MAIA III TESCAN and JEOL JSM-6701F) were employed.

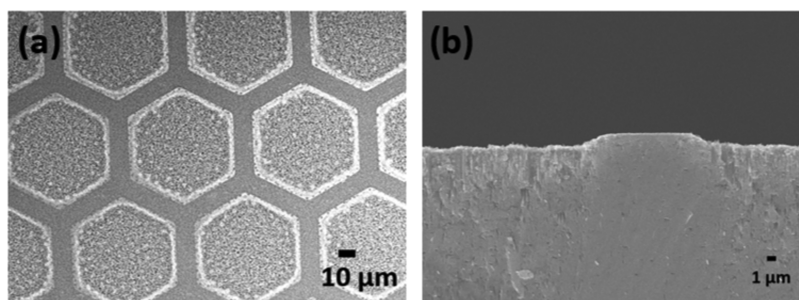


**Figure 3.** (a) Top-view and (b) cross-section of MACE results from the Si/5 nm Ag with an etching time of 90 min. The etchant consists of an aqueous solution of 5.3 M HF and 0.42 M H<sub>2</sub>O<sub>2</sub>.

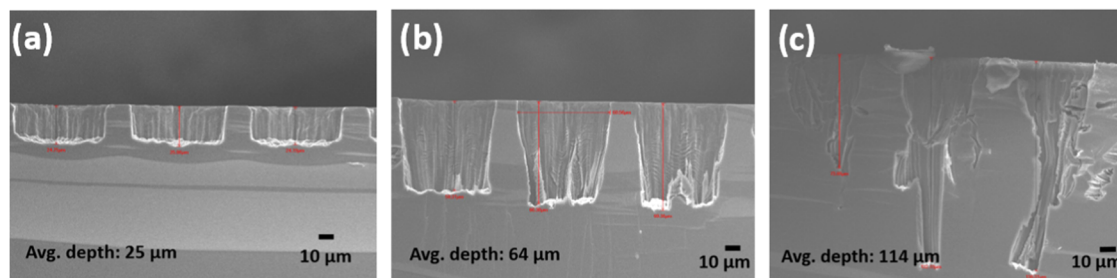


**Figure 4.** MACE results of the metal bilayer Si/5 nm Ag/10 nm Au. The etchant consists of an aqueous solution of 8 M HF and 0.2 M H<sub>2</sub>O<sub>2</sub>, and the etching times were (a) 3 h, (b) 6 h, and (c) 9 h.

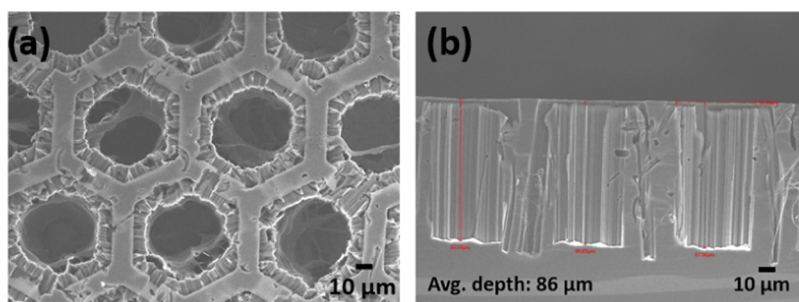


**Figure 5.** (a) Top-view and (b) cross-sectional of MACE results from a single metal layer Si/10 nm Au with an etching time of 3 h. The etchant consists of an aqueous solution of 8 M HF and 0.2 M H<sub>2</sub>O<sub>2</sub>.

### 3. RESULTS AND DISCUSSION

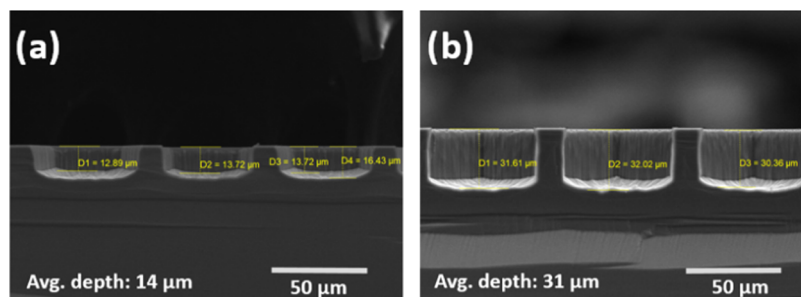
**3.1. Effect of an Ultrathin Metal Film.** To apply the MACE process to Si micromachining, the mass transfer of the etched material at the metal/Si interface should be promoted, as mentioned above. In the relatively thick metal layer of 20 nm or thicker commonly used in most MACE processes, only in-plane mass transfer is possible, and so the mass transfer is inevitably limited. In this study, an ultrathin metal layer (5–10 nm) was used to promote the out-of-plane mass transfer, enabling uniform etching in the entire area of the micropattern.

Figure 3 shows the MACE results with the ultrathin Ag films (5 nm). Ag is one of the most widely used metal materials in MACE. In the case of the ultrathin Ag film, the film is composed of unconnected nanoparticles, and when the MACE process is performed, these nanoparticles appear to penetrate the Si substrate and form a porous layer. In addition, a substantial amount of Ag itself may be corroded. The standard potential ( $E^\circ$ ) of Ag is 0.80 V; thus, Ag can be easily oxidized and dissolved by the oxidizing agent H<sub>2</sub>O<sub>2</sub> ( $E^\circ = 1.76\text{V}$ ). A single Ag thin film has been previously used for nanostructure fabrication but is not suitable for deep etching of Si microstructures.

A Ag/Au bimetallic thin film was tested to compensate for the instability of a single Ag thin film. Kim et al. found that the Au/Ag bilayer configuration had benefits in that a thin Ag layer promotes adhesion.<sup>12</sup> Figure 4 shows the results of the MACE process for the Si/5 nm Ag/10 nm Au. Compared to the case of a single Ag thin film, the etching result is relatively improved. The porous layer formation is not observed, and the original pattern shape is mostly maintained even after a long period of etching for more than 6 h. Since Au ( $E^\circ = 1.83\text{V}$ ) is much more stable than Ag, the upper Au thin film seems to protect the lower Ag layer from corrosion. However, as the etching time increases, the diameter of the metal pattern becomes shrunk, and porous defects begin to appear. The Ag thin film layer is presumed to be gradually corroded over time and peeled off with the upper Au thin film.

It was assessed that even the Ag/Au bimetallic thin film was not suitable for the MACE process for a long time due to its instability and the formation of porous defects. Therefore, the MACE process using a single Au thin film was attempted. (Figure 5) In the case of a single Au thin film, the size of the original metal pattern was well maintained even after deep etching, and the etching rate was faster than that of a single Ag





**Figure 6.** MACE results of Si/10 nm Au from different solvents: (a) water/ethanol (2:8 v/v) and (b) pure ethanol. The etchant contains 8 M HF and 0.2 M  $\text{H}_2\text{O}_2$ . The etching time for all samples was 3 h.

thin film or Au/Ag bimetallic thin film. This is due to the stability of the Au thin film. Nevertheless, porous defects were observed after the MACE process. It is presumed that when the etching byproducts generated at the bottom of the hole diffuse to the top, some of them are adsorbed to the inner wall and create porous defects on the inner wall.

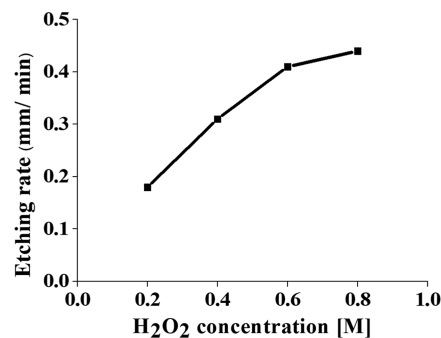
**3.2. Effect of Solvent.** When a single Au thin film was used, the stability of the thin metal film was improved, but the problem of the generation of porous defects remained. To solve this problem, a solvent other than water was tested. According to previous reports, porous defect formation could be minimized by adding ethanol to the etching solution.<sup>13</sup>

Figure 6 shows the effect of the addition of ethanol to the etch profile. The etch profile was significantly improved with ethanol addition compared to a pure aqueous solution. No porous defect formation was observed either on the inner wall or the bottom of the hole. On the other hand, the etching rate was decreased compared to pure water, probably because the viscosity of the solution increases when ethanol is added, which slows down the mass transfer.

The reason for the excellent etch profile in the ethanol solvent is not clearly understood yet. One possibility is that ethanol is much less polar than water, and thus the corrosion and dissolution of the metal layer are minimized. In this case, it is possible to prevent the metal catalyst from readsorbing on the inner wall of the hole and acting as seeds for the pore formation reaction.

**3.3. Maximization of the Etch Rate and Prolonged Etching.** Compared to the conventional Si dry etching method (DRIE), MACE wet etching has a considerably slower etching rate, and so it is necessary to increase the MACE etching rate. The etching rate can be optimized mainly by controlling the concentration of the oxidizing agent  $\text{H}_2\text{O}_2$  in the etching solution.<sup>14</sup> Figure 7 shows the MACE etching results according to the  $\text{H}_2\text{O}_2$  concentration. As expected, the etching rate increased as the concentration of  $\text{H}_2\text{O}_2$  increased, but the etching rate was saturated at  $[\text{H}_2\text{O}_2] = \sim 0.8$  M. This implies that the etch rate might be influenced by the concentration gradient as the etching solution is unstirred. Even at a fast etching rate, the etch profile after MACE etching showed an excellent cross-sectional profile (Figure S1). However, we observed that porous layers begin to form on the top portion of the etched structure after the prolonged etch time (see Figure S3). So, we found that the optimized  $[\text{H}_2\text{O}_2]$  is  $\sim 0.4$  M.

As the MACE process parameters have been optimized for microstructures, deep etch was performed for a long time using the optimized conditions. As shown in Figure 8, the prolonged etch exhibits a uniform etch rate for 10 h or longer. This



**Figure 7.** Graph of the etching rate as a function of  $\text{H}_2\text{O}_2$  concentration. The etching rate increased as the concentration of  $\text{H}_2\text{O}_2$  increased. The etchant consists of an ethanolic solution of 8 M HF.

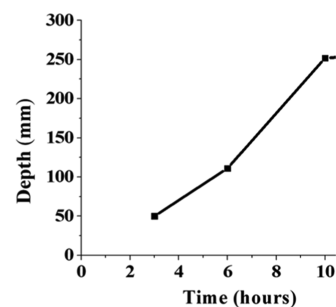


**Figure 8.** Deep MACE results showing etching depth as a function of the etch time. The etchant consists of an ethanolic solution of 8 M HF and 0.4 M  $\text{H}_2\text{O}_2$ .

indicates little corrosion of metal catalyst even during deep etch, and mass transfer from the bottom of the deep hole proceeds uniformly. A smooth etch profile is fabricated even after prolonged etching, and no porous defects were observed (Figure S2). Since the thickness of an ordinary Si wafer is 100–400  $\mu\text{m}$ , it is also possible to fabricate even a through-hole on the Si substrate by the deep MACE process developed in this study.<sup>15</sup>

The etch profile fabricated by the optimized deep etch condition is shown in Figure 9. After about 10 h of etching, a deep hole exceeding 200  $\mu\text{m}$  was produced with a very smooth and vertical ( $>85^\circ$ ) profile. We note that the wall thickness at the upper part is somewhat smaller than that at the bottom, which can be attributed to the remote etching in MACE. That is, although most of the etching proceeds in the shallow area of the Si–metal contact, some of the injected holes diffuse out and reach the upper part of the structure, leading to the thinning of the Si wall.<sup>16,17</sup>

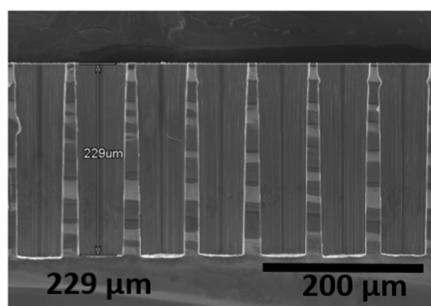


**Figure 9.** MACE results of Si/10 nm Au with an etching time of 10 h. The etchant consists of an ethanolic solution of 8 M HF and 0.4 M H<sub>2</sub>O<sub>2</sub>.

#### 4. CONCLUSIONS

A deep etching method of micropatterns on Si based on metal-assisted chemical etching was successfully developed, which was impossible with the common MACE process. In this deep MACE, the critical improvement was to promote the out-of-plane mass transfer at the metal/Si interface using an ultrathin metal film. In addition, it was found that when ethanol was used as a solvent instead of water, the formation of porous defects was suppressed. Under these optimized deep etch conditions, very deep (>200 μm) and vertical (>85°) holes could be etched at a fast etch rate (>0.4 μm/min). We take these results as evidence for the out-of-plane mass transfer because the conventional MACE (having a thick metal film with a laterally micrometer-sized dimension) exhibits an order of magnitude slower etch rate (~0.02 μm/min) and nonuniform etch profile.<sup>7</sup> Using this new deep MACE process, various structures required for MEMS devices or biosensors will be manufactured at a very low cost and on a large scale.

#### ■ ASSOCIATED CONTENT

##### SI Supporting Information

The Supporting Information is available free of charge at <https://pubs.acs.org/doi/10.1021/acsomega.2c01113>.

Additional SEM images of cross-sectional and top-view etched structures (PDF)

#### ■ AUTHOR INFORMATION

##### Corresponding Author

**Ilwhan Oh** – Departments of Applied Chemistry and Department of Energy Convergence Engineering, Kumoh National Institute of Technology, Gumi, Gyeongbuk 39177, South Korea; [orcid.org/0000-0002-5424-0777](https://orcid.org/0000-0002-5424-0777); Email: [ioh@kumoh.ac.kr](mailto:ioh@kumoh.ac.kr)

##### Author

**Anafi Nur'aini** – Chemical Engineering and Department of Energy Convergence Engineering, Kumoh National Institute of Technology, Gumi, Gyeongbuk 39177, South Korea; [orcid.org/0000-0002-8261-7703](https://orcid.org/0000-0002-8261-7703)

Complete contact information is available at:

<https://pubs.acs.org/doi/10.1021/acsomega.2c01113>

##### Notes

The authors declare no competing financial interest.

#### ■ ACKNOWLEDGMENTS

I.O. acknowledges the support from the National Research Foundation (NRF) of Korea (NRF-2020R1F1A1072515).

#### ■ REFERENCES

- (1) Madou, M. J. *Fundamentals of Microfabrication and Nanotechnology*; CRC Press, 2018. DOI: [10.1201/9781315274164/FUNDAMENTALS-MICROFABRICATION-NANOTECHNOLOGY-THREE-VOLUME-SET-MARC-MADOU](https://doi.org/10.1201/9781315274164/FUNDAMENTALS-MICROFABRICATION-NANOTECHNOLOGY-THREE-VOLUME-SET-MARC-MADOU).
- (2) Zhang, X. *Electrochemistry of Silicon and Its Oxide*; Kluwer Academic Publishing, 2004.
- (3) Cozzi, C.; Polito, G.; Kolasinski, K. W.; Barillaro, G. Controlled Microfabrication of High-Aspect-Ratio Structures in Silicon at the Highest Etching Rates: The Role of H<sub>2</sub>O<sub>2</sub> in the Anodic Dissolution of Silicon in Acidic Electrolytes. *Adv. Funct. Mater.* **2017**, *27*, No. 1604310.
- (4) Huang, Z.; Geyer, N.; Werner, P.; de Boor, J.; Gösele, U. Metal-Assisted Chemical Etching of Silicon: A Review. *Adv. Mater.* **2011**, *23*, 285–308.
- (5) Han, H.; Huang, Z.; Lee, W. Metal-Assisted Chemical Etching of Silicon and Nanotechnology Applications. *Nano Today* **2014**, *9*, 271–304.
- (6) Huo, C.; Wang, J.; Fu, H.; Li, X.; Yang, Y.; Wang, H.; Mateen, A.; Farid, G.; Peng, K.-Q. Metal-Assisted Chemical Etching of Silicon in Oxidizing HF Solutions: Origin, Mechanism, Development, and Black Silicon Solar Cell Application. *Adv. Funct. Mater.* **2020**, *30*, No. 2005744.
- (7) Geyer, N.; Fuhrmann, B.; Huang, Z.; de Boor, J.; Leipner, H. S.; Werner, P. Model for the Mass Transport during Metal-Assisted Chemical Etching with Contiguous Metal Films as Catalysts. *J. Phys. Chem. C* **2012**, *116*, 13446–13451.
- (8) Li, L.; Liu, Y.; Zhao, X.; Lin, Z.; Wong, C. P. Uniform Vertical Trench Etching on Silicon with High Aspect Ratio by Metal-Assisted Chemical Etching Using Nanoporous Catalysts. *ACS Appl. Mater. Interfaces* **2014**, *6*, 575–584.
- (9) Song, Y.; Ki, B.; Choi, K.; Oh, I.; Oh, J. In-Plane and out-of-Plane Mass Transport during Metal-Assisted Chemical Etching of GaAs. *J. Mater. Chem. A* **2014**, *2*, 11017–11021.
- (10) Volovlikova, O.; Silakov, G.; Gavrilov, S.; Maniecki, T.; Dudin, A. Investigation of the Pd Nanoparticles-Assisted Chemical Etching of Silicon for Ethanol Solution Electrooxidation. *Micromachines* **2019**, *10*, No. 872.
- (11) Li, X.; Bonn, P. W. Metal-Assisted Chemical Etching in HF/H<sub>2</sub>O<sub>2</sub> Produces Porous Silicon. *Appl. Phys. Lett.* **2000**, *77*, 2572–2574.
- (12) Kim, S. M.; Khang, D. Y. Bulk Micromachining of Si by Metal-Assisted Chemical Etching. *Small* **2014**, *10*, 3761–3766.
- (13) Miao, B.; Zhang, J.; Ding, X.; Wu, D.; Wu, Y.; Lu, W.; Li, J. Improved Metal Assisted Chemical Etching Method for Uniform, Vertical and Deep Silicon Structure. *J. Micromech. Microeng.* **2017**, *27*, No. 055019.
- (14) Zahedinejad, M.; Farimani, S. D.; Khaje, M.; Mehrara, H.; Erfanian, A.; Zeinali, F. Deep and Vertical Silicon Bulk Micromachining Using Metal Assisted Chemical Etching. *J. Micromech. Microeng.* **2013**, *23*, No. 055015.
- (15) Cruz, S.; Hönig-d'Orville, A.; Müller, J. Fabrication and Optimization of Porous Silicon Substrates for Diffusion Membrane Applications. *J. Electrochem. Soc.* **2005**, *152*, C418.
- (16) Tamarov, K.; D Swanson, J.; A Unger, B.; W Kolasinski, K.; T Ernst, A.; Aindow, M.; Lehto, V.-P.; Riikonen, J. Controlling the Nature of Etched Si Nanostructures: High- versus Low-Load Metal-Assisted Catalytic Etching (MACE) of Si Powders. *ACS Appl. Mater. Interfaces* **2020**, *12*, 4787–4796.
- (17) Kolasinski, K. W.; Tamarov, K.; Kiviluoto, R.; Swanson, J. D.; Unger, B. A.; Ernst, A. T.; Aindow, M.; Riikonen, J.; Lehto, V. P. Low-Load Metal-Assisted Catalytic Etching Produces Scalable Porosity in Si Powders. *ACS Appl. Mater. Interfaces* **2020**, *12*, 48969–48981.